



Chemical Characterization of Sub-micron Aerosols during New Particle Formation in an Urban Atmosphere

Vijay P. Kanawade^{1,2*}, Sachchida N. Tripathi^{2*}, Abhishek Chakraborty^{2,3}, Huan Yu⁴

¹ University Centre for Earth, Ocean and Atmospheric Sciences, University of Hyderabad, Telangana 500046, India

² Department of Civil Engineering and Centre for Environmental Science and Engineering, Indian Institute of Technology Kanpur, Kanpur 208016, India

³ Environmental Science and Engineering Department, Indian Institute of Technology, Bombay, Mumbai 40076, India

⁴ Department of Atmospheric Science, School of Environmental Studies, China University of Geosciences, Wuhan 430074, China

ABSTRACT

While high concentrations of pre-existing particles tend to inhibit new particle formation (NPF) in the atmosphere, severely polluted megacities around the world are becoming hot spots for the latter. We measured the particle number-size distributions with a Scanning Mobility Particle Sizer (SMPS) in the urban environment of Kanpur, India, and discovered that particle bursts occurred on 82% of the observation days, indicating that new particles frequently formed from gaseous precursors despite the relatively high concentrations of pre-existing particles. During such events, Aitken-mode particles contributed more than 50% of the total particle mass. Additionally, we used a high-resolution time-of-flight aerosol mass spectrometer (HR-ToF-AMS) to assess chemical changes in the sub-micron particles during NPF events. Because the HR-ToF-AMS can not detect particles smaller than 40 nm in diameter, however, it was not possible to investigate the chemistry driving the NPF. Our results indicated that oxygenated organic aerosols (OAs) constituted almost 77%—the largest fraction—of the sub-micron particles. The m/z 57 ion ($C_4H_9^+$), a tracer of hydrocarbon-like OA (HOA), displayed significantly enhanced signal intensity during all of the NPF event days. Moreover, the increased proportion of organic ions, m/z 44 (CO_2^+), on these days suggested the presence of less volatile, highly oxidized OAs (LV-OOAs), revealing that the growth of new particles was mainly due to the condensation of low-volatility organic species. The substantially elevated signal intensity of amines (viz., CHN^+ , CH_4N^+ , $C_2H_4N^+$, $C_3H_8N^+$, and $C_5H_{12}N^+$) in the sub-micron aerosols during NPF further demonstrated that these nitrogen-containing organic compounds may have played a critical role in these events. Thus, our findings emphasize the relevance of amines to secondary aerosol formation in severely polluted urban environments.

Keywords: Nucleation; Growth; Amines; Urban areas.

INTRODUCTION

Atmospheric ultrafine particles (typically diameter < 100 nm) have been the topic of immense attention since last two decades as it constitutes the largest fraction of the total particle number and mass budgets on a global scale (Kulmala *et al.*, 2004; Spracklen *et al.*, 2006). The major sources of ultrafine particles include direct emission (e.g., vehicular exhaust, biomass burning and industrial processes; Seigneur, 2009) and secondary aerosol formation (as a result of gas-to-particle conversion processes referred to as *aerosol nucleation*; Zhang *et al.*, 2012; Kulmala *et al.*, 2013). The fraction of these

newly formed particles may activate to cloud condensation nuclei (CCN) and ice nuclei (IN), in turn affecting cloud macro- and microphysical (Andreae and Rosenfeld, 2008; Sarangi *et al.*, 2018) and precipitation properties (Zhang *et al.*, 2007; Sarangi *et al.*, 2017) on a regional to global scale. However, the modelling of CCN from anthropogenic aerosol sources in global climate models (Prenni *et al.*, 2001; Spracklen *et al.*, 2008; Pierce and Adams, 2009) is largely hindered by our limited understanding of secondary aerosol formation processes. The high concentration of anthropogenic ultrafine particles was also recently linked to respiratory hospitalizations in cities (Samoli *et al.*, 2016).

Highly polluted cities, especially in developing nations like India and China, are becoming hot spots of new particle formation (NPF) (Yu *et al.*, 2017). In urban environments, sulfate, nitrate and organics were all shown to influence the growth of ultrafine particles (Smith *et al.*, 2010; Bzdek *et al.*, 2012; Salimi *et al.*, 2015; Yu *et al.*, 2017). Tao *et al.* (2016) recently showed that heterogeneous uptake of

* Corresponding author.

E-mail address:

vijaykanawade03@yahoo.co.in (V.P. Kanawade);
snt@iitk.ac.in (S.N. Tripathi)

amines via acid-base reactions can also contribute to particle growth during the NPF. Urban environments often experience severe air pollution episodes, owing to secondary aerosol formation from the atmospheric chemical processing of aerosol precursors. The long-range transported polluted plumes with elevated sulfuric acid concentrations (H_2SO_4) via oxidation of sulfur dioxide (SO_2) can also influence the growth of ultrafine particles in remote locations (Creamean *et al.*, 2011). Recent laboratory experiments showed that coupling between H_2SO_4 and large oxidized organic compounds is involved in both the formation and growth of ultrafine particles under ambient conditions (Schobesberger *et al.*, 2013). A recent study showed that the H_2SO_4 -dimethylamine- H_2O ternary nucleation system was able to explain the high NPF rates in an urban atmosphere of Shanghai, China (Yao *et al.*, 2018). Previous measurements in diverse environments also detected dimethyl- and diethyl-aminium salts (DMA^+ and DEA^+) in accumulation-mode particles collected during NPF events, such as Finland boreal forests (Mäkelä *et al.*, 2003), downwind of the major bovine source (Sorooshian *et al.*, 2008), marine air masses (Facchini *et al.*, 2008), and urban areas (Sorooshian *et al.*, 2007; Setyan *et al.*, 2014). Several other studies have also indicated base compounds, associated with neutralization of H_2SO_4 , contribute to the growth of ultrafine particles (Zhang *et al.*, 2004; Smith *et al.*, 2010; Bzdek *et al.*, 2011; Kirkby *et al.*, 2011; Dawson *et al.*, 2012; Almeida *et al.*, 2013). Laboratory experiments have further shown that amines have a greater impact on NPF than ammonia by clustering with and/or stabilizing H_2SO_4 clusters (Murphy *et al.*, 2007; Kurtén *et al.*, 2008; Erupe *et al.*, 2011; Yu *et al.*, 2012; Almeida *et al.*, 2013; Jen *et al.*, 2014; Kürten *et al.*, 2014). Numerical simulations also demonstrated that amines have a great ability in enhancing NPF rates even at low amine concentrations (few pptv) over the major source regions (Yu and Luo, 2014) and may further affect secondary organic aerosol production via acid-base chemistry (Murphy *et al.*, 2007).

A recent study in the Indian Institute of Technology (IIT) Kanpur campus (hereafter referred to as *IITK*) showed that NPF occurs commonly in Kanpur (Kanawade *et al.*, 2014c), even in the presence of high aerosol loading (Kanawade *et al.*, 2014b). There are more than ten studies reporting the systematic characteristics of NPF events in India (Mönkkönen *et al.*, 2005; Hyvärinen *et al.*, 2010; Moorthy *et al.*, 2011; Neitola *et al.*, 2011; Siingh *et al.*, 2013; Kanawade *et al.*, 2014a, b, c; Sobhan Kumar *et al.*, 2014; Kamra *et al.*, 2015; Babu *et al.*, 2016; Leena *et al.*, 2017), but size-resolved chemical composition of sub-micron aerosols during the NPF remains largely unknown. Here, we analyzed simultaneous measurements of the particle number-size distribution (PNSD) in the size range of 4.45–736.5 nm from TSI Scanning Mobility Particle Sizer (SMPS) and size-resolved chemical composition from Aerodyne high-resolution time-of-flight aerosol mass spectrometer (hereafter referred to as *AMS*). The main aim of this study is to provide some insights into the chemical composition of sub-micron aerosols during the NPF events in an urban atmosphere.

METHODS

We carried out aerosol measurements (via SMPS and AMS) at about 10 m above the ground at the IITK site (26.46° N, 80.32° E, 125 m a.m.s.l.) during 30 March–15 April 2013 (Fig. S1). Details of the sampling site, aerosol sampling (SMPS) procedures and data reduction methodologies are given elsewhere (Kanawade *et al.*, 2014c). Briefly, we obtained PNSD in the size range of 4.45–736.5 nm using a set of two SMPS systems; a Long Differential Mobility Analyzer (LDMA; Model 3080; TSI Inc.) in combination with a butanol condensation particle counter (CPC; Model 3775; TSI Inc.), and a Nano DMA (NDMA; Model 3085; TSI Inc.) with a butanol CPC (Model 3776; TSI Inc.), yielding one average PNSD at every 5 min time interval. The mode diameter (i.e., local maximum of the particle size distribution) was obtained by fitting a lognormal distribution to the measured particle size distribution. Then, we calculated the particle growth rate (GR) during the NPF events by fitting a first-order polynomial line through the temporal evolution of the particle mode diameter ($D_{m, \text{mode}}$) and calculating its slope (Dal Maso *et al.*, 2005). The coagulation sink (CoagS) determines how rapidly small particles are removed through coagulation by larger particles. CoagS matrix was calculated for all sizes (142 size bins) in the size range of 4.45–736.5 nm based on the Kulmala *et al.* (2001) approach and then total CoagS was obtained. We measured trace gases (NO_x , SO_2 , O_3 and CO) and meteorological parameters (temperature, relative humidity, wind speed, and wind direction) simultaneously in the vicinity of aerosol measurement site (Fig. S1). The Thermo Scientific (USA) gas analyzers were installed in an air-conditioned laboratory on the top of an existing overhead water tank of 25 m height from the ground level, which was located about 50 m to the south of the aerosol instruments' site. SO_2 was measured using a pulsed fluorescence analyzer (Model 43*i*), with a minimum detection limit of < 0.5 ppb. NO_x is measured using a chemiluminescence analyzer (Model 42*i*), with a minimum detection limit of 0.4 ppb. O_3 was measured using UV absorption analyzer (Model 49*i*), with a minimum detection limit of 1.0 ppb. CO was measured using a non-dispersive infrared gas filter correlation technique (Model 48*i*), with a minimum detection limit of 40.0 ppbv. The daily zero settings and weekly span checks were conducted for the best performance of gas analyzers. Meteorological parameters were measured simultaneously at the Indian Space Research Organization (ISRO)'s automatic weather station (AWS-ES, ISRO20) installed inside the IITK campus, which is located at about 250 m to the north of the aerosol measurement site. Further details on gas analyzers and meteorological instruments can be found elsewhere (Gaur *et al.*, 2014).

We used an Aerodyne AMS to quantify the mass concentrations of non-refractory species including ammonium, sulfate, nitrate, chloride and total organic matter via thermal vaporization (typically at 600°C) and 70 eV electron-impact ionization (DeCarlo *et al.*, 2006; Canagaratna *et al.*, 2007). The AMS was run alternatively in V- and W-modes (time-averaged mass resolution of 2903 and 4089 at m/z 184, respectively), each with 1 minute sampling time. Due to a

hard mirror malfunction, the W-mode data are not continuous. Therefore, we considered only the V-mode data in this study. We have calibrated the AMS for both the inlet flow and particle sizing at the beginning of measurements. We have also performed ionization efficiency calibration before, during, and after the measurements following standard protocols (Jimenez *et al.*, 2003). Positive Matrix Factorization (PMF) analysis of organic HR mass spectra (m/z 12–300, V-mode) was carried out using the PMF v2.06 evaluation tool (Ulbrich *et al.*, 2009; see supplementary text). More details on the AMS sampling procedures and data reduction methodologies can be found elsewhere (Chakraborty *et al.*, 2015).

RESULTS AND DISCUSSION

Identification of New Particle Formation Events

Fig. 1 shows the temporal evolution of PNSDs, particle mode diameter, number concentration of nucleation-mode particles (N_{4-20}) and total particles, CoagS, aerosol composition fractions from AMS, meteorological parameters (temperature, relative humidity, wind speed, wind direction, and solar radiation), and trace gases (SO_2 , NO_x , O_3 and CO).

The regional NPF occurs in two distinct stages: i) formation of nanometer-sized critical clusters (i.e., 1–2 nm) from gaseous vapors and ii) subsequent growth of these stable clusters to large sizes by condensable vapors and/or particle-particle

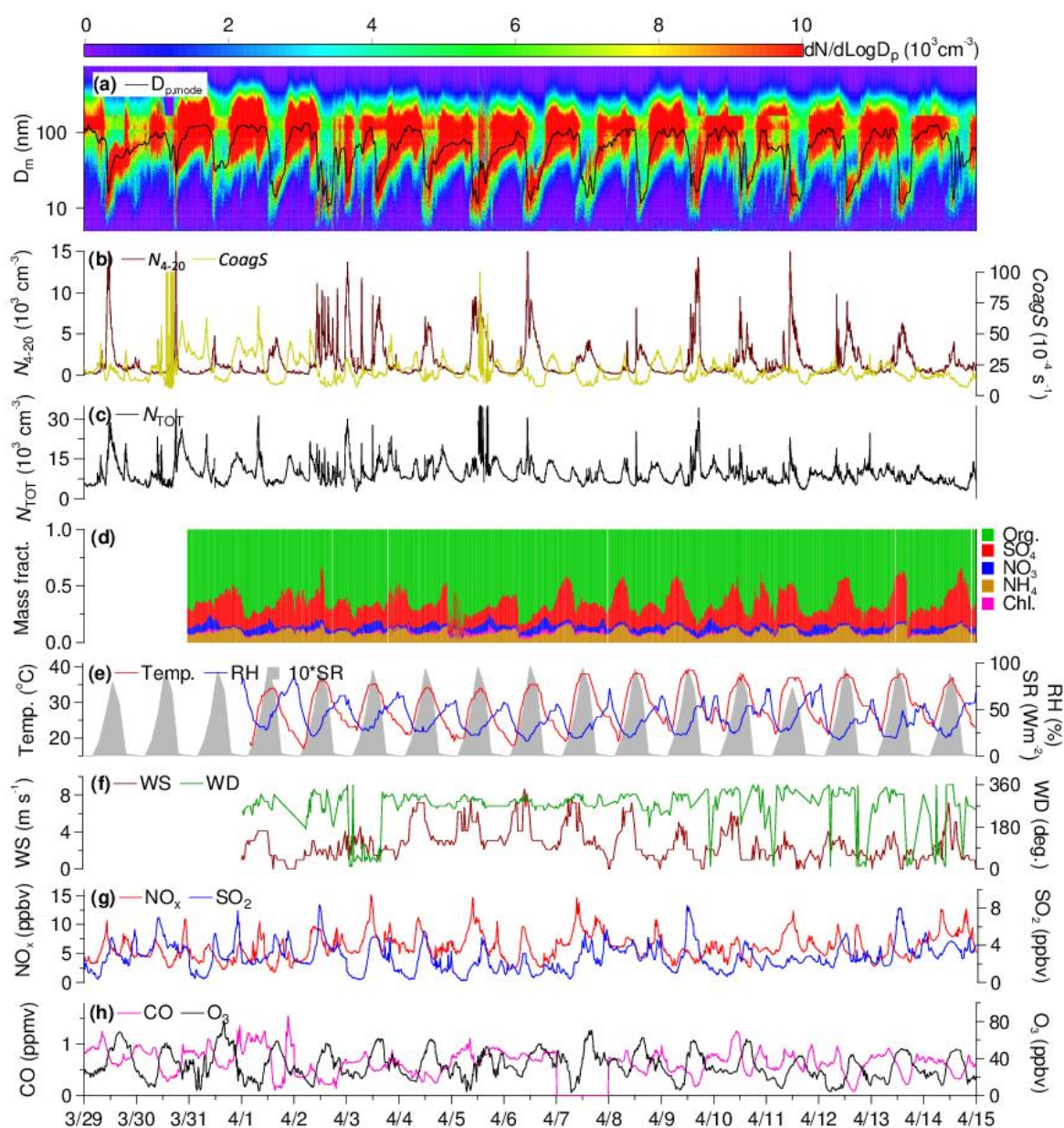


Fig. 1. Time evolution of (a) particle number-size distributions and particle mode diameter ($D_{p, mode}$); (b) number conc. of nucleation-mode particles (N_{4-20}) and coagulation sink (CoagS); (c) total particle number concentration; (d) aerosol composition fraction from AMS; (e) temperature, relative humidity and solar radiation; (f) wind speed and wind direction; (g) NO_x and SO_2 ; and (h) CO and O_3 at the IITK site during March–April 2013.

coagulation (Kulmala *et al.*, 2013). Here, NPF event is identified by the presence of a distinctly new mode of particles less than 20 nm diameter size with a steady growth in particle size over at least 6 hours, thus particle number-size distributions appearing as conventional noontime “banana-shaped” aerosol size growth. Particle bursts in the lower size range (4–20 nm) occurred on 14 days out of total 17 sampled days (i.e., 82% of all observation days). NPF events are then classified into four types; *strong* (Type-I) and *moderate to weak* (Type-II), depending on the net rate of increase in N_{4-20} during the first hour of the event. The net rate of increase in N_{4-20} (dN_{4-20}/dt) larger than 10,000 particles $\text{cm}^{-3} \text{h}^{-1}$ identifies *strong* events whereas dN_{4-20}/dt smaller than 10,000 particles $\text{cm}^{-3} \text{h}^{-1}$ identifies *moderate to weak* events. The *Aitken-mode particle growth* events and broken “banana-shaped” aerosol size growth events were put into Type-III whereas *non-NPF* events were assigned to Type-IV. Type-I events were observed on 3 consecutive days (4–6 April) whereas Type-II events were observed on 29 March and 7, 11, 12 and 13 April (5 days). Type-III events were observed on 1, 2, 3, 8, 9 and 10 April (6 days) whereas Type-IV events were observed on 30, 31 March and 14 April (3 days). Note that AMS measurements were not available on 29–30 March. A recent study at the same site has performed the detailed analysis of different types of NPF events using six weeks of measurements (Kanawade *et al.*, 2014c).

It is important to note that the AMS cannot detect particles smaller than 40 nm, below which particle nucleation and early growth occurs. Given this limitation, AMS measurements are not suitable to assess the chemistry driving NPF, which is not the focus of this study. However, the AMS measurements are still extremely useful to examine chemical composition of sub-micron aerosols during the NPF events and also the data obtained can be attributed to the growth of particles several hours after the nucleation (i.e., < 3 nm cluster formation) (Creamean *et al.*, 2011; Setyan *et al.*, 2014). The derived particle growth (GR) varied from 3.2 to 6.7 nm h^{-1} during the NPF events. With these growth rates, the significant fraction of newly formed particles (particularly on Type-I NPF event days) would eventually grow larger than the lowest detectable size by AMS within few hours after the nucleation, i.e., during afternoon hours when the photochemistry is at its peak. To establish this, we have calculated number concentration of particles of size between 40 nm and 100 nm, and compared with N_{4-20} (Fig. S2). The rate of change in N_{4-20} is well captured by the subsequent rate of change in N_{40-100} , suggesting that the major fraction of nucleation-

mode particles grew over the lowest detectable size of the AMS (i.e., 40 nm). There was no rain reported and sky was almost clear during the entire study period. The diurnal pattern of temperature and relative humidity did not change during the entire time period. The wind speed stayed mostly around 7 m s^{-1} , and the prevailing wind direction was northwest. NO_x showed usual early morning peak, whereas SO_2 showed sharp increase in the morning hours and minor enhancements during evening hours, associated with the traffic hours. The O_3 concentrations were highest during the noontime when the photochemistry is at its peak.

Table 1 shows the summary statistics of particle number concentrations in different size modes for the entire observation period. The number concentrations of nucleation-mode particles varied from 59 to $24.64 \times 10^3 \text{ cm}^{-3}$, with a mean and standard deviation values of $2.0 \times 10^3 \pm 2.75 \times 10^3 \text{ cm}^{-3}$. The mean nucleation-mode particle concentrations were lower as compared to the observed at other semi-urban to urban sites (e.g., Wehner and Wiedensohler, 2003; Stanier *et al.*, 2004; Wu *et al.*, 2008; Kanawade *et al.*, 2012) as well as regional background sites (e.g., Shen *et al.*, 2011; Németh *et al.*, 2018), but higher than remote sites in India (Moorthy *et al.*, 2011; Kanawade *et al.*, 2014a). The number concentrations of Aitken-mode particles varied from 1.23×10^3 to $30.23 \times 10^3 \text{ cm}^{-3}$, with mean and standard deviation values of $5.27 \times 10^3 \pm 2.81 \times 10^3 \text{ cm}^{-3}$. Several studies reported the higher Aitken-mode than nucleation-mode particle number concentrations, particularly in urban environments (e.g., Hussein *et al.*, 2004; Wu *et al.*, 2008; Kanawade *et al.*, 2014c), because Aitken-mode particles not only constitute the grown freshly nucleated particles but also the primary emissions mainly from fossil- and bio-fuel combustion. The number concentration of accumulation-mode particles varied from 0.76×10^3 to $12.78 \times 10^3 \text{ cm}^{-3}$, with a mean and standard deviation values of $2.99 \times 10^3 \pm 1.58 \times 10^3 \text{ cm}^{-3}$. The ratio of Aitken-mode to accumulation-mode particles was 1.76, which is not surprising as newly formed particles can efficiently grow to Aitken-mode size and only a small fraction can reach size as large as accumulation mode (> 100 nm). The ratio value is within the range reported by previous studies at semi-urban and urban sites in India (Hyvärinen *et al.*, 2010; Kanawade *et al.*, 2014b). Overall, Aitken-mode particle number was higher than nucleation- and accumulation-mode particles.

Source Apportionment of Organic Aerosols

We performed Positive Matrix Factorization analysis on the organic HR mass spectra of AMS to investigate the sources and processes of organic aerosol (OA) during the

Table 1. Summary statistics of number concentration of particles in different size modes.

	Nucleation	Aitken	Accumulation	Total
Diameter range (nm)	4.45–20	20–100	100–736.5	4.45–736.5
Mean (cm^{-3})	2,021	5,266	2,991	10,195
Standard deviation	2,757	2,819	1,589	4,612
Median (cm^{-3})	903	4,573	2,678	9,115
Minimum (cm^{-3})	59	1,234	763	2,811
Maximum (cm^{-3})	24,644	30,230	12,777	54,318
Contribution (%)	19.8	51.6	29.3	100

observation period. PMF diagnostics with 1–4 factors and f_{peak} values ranging from -5 to $+5$, to get 3% change (Zhang *et al.*, 2011) over the minimum Q/Q_{exp} value for each factor, and the corresponding residual are presented in Fig. S3. Here, we used an “Improved-Ambient” elemental analysis method for the AMS mass spectra (Canagaratna *et al.*, 2015). We determined 4 distinct factors namely: biomass burning OA (BBOA; $O/C = 0.46$), hydrocarbon-like OA (HOA; $O/C = 0.06$) mainly associated with local primary emissions, and two types of oxygenated OA (OOA; OOA-1 and OOA-2, $O/C = 0.72$ and 0.55 , respectively) (Fig. S4).

The PMF analysis showed that oxygenated organic aerosols constituted the largest fraction of sub-micron aerosols followed by hydrocarbon-like OA and biomass burning OA during entire observation period (Fig. 2). m/z 57 ion ($C_4H_9^+$) has been identified as a tracer of HOA and largely associated with combustion-generated primary aerosols from traffic (Zhang *et al.*, 2005; Canagaratna *et al.*, 2010), whereas m/z 60 ($C_2H_4O_2^+$) and m/z 73 ($C_3H_5O_2^+$) ions have been shown to be tracers of BBOA and associated with a mixture of both biomass burning and cooking aerosols (Aiken *et al.*, 2009). We have calculated fractions of these variables relative to OA mass (f_{HOA} , f_{57} , f_{60} , and f_{73}) to examine traffic- and/or biomass-burning-emitted OA during the observed NPF events. Fig. 3 shows time evolution of fractions f_{HOA} , f_{57} , f_{60} and f_{73} during entire observation period. f_{60} and f_{73} showed typical diurnal variation, with higher concentrations during nighttime than daytime, owing to near-surface sources and dilution effect. In contrast, f_{57} and f_{HOA} showed elevated diurnal pattern. The traffic rush-hour enhancements in

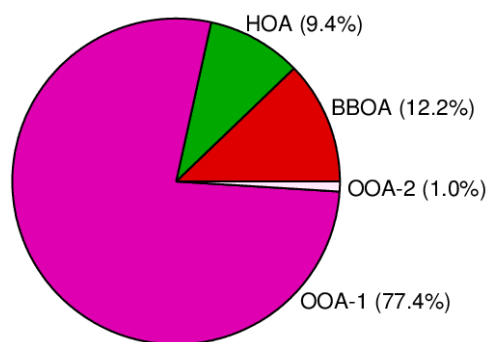


Fig. 2. Percentage of total OA obtained from the PMF analysis of the HR mass spectra for the time period of 12:00–18:00 local time during the observation period.

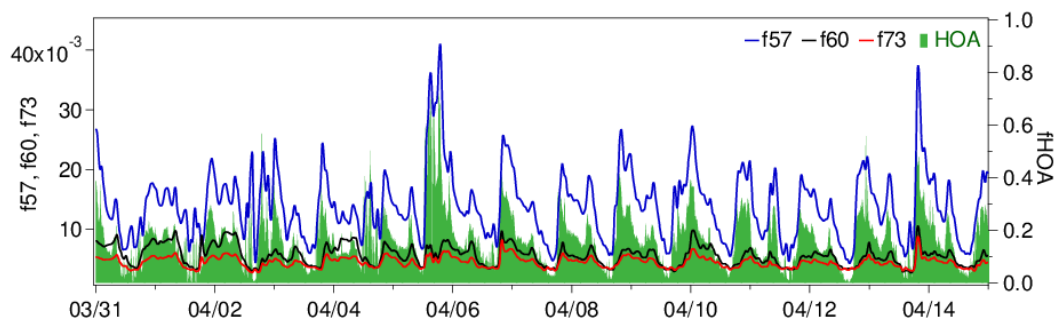


Fig. 3. Time evolution of fractions f_{57} , f_{60} , f_{73} , and f_{HOA} during the entire observation period.

both f_{57} and f_{HOA} are clearly visible. The f_{57} and f_{HOA} were significantly elevated on 5 April (Type-I NPF event), suggesting the possible source of combustion-generated primary OAs. A very good correlation between f_{57} and f_{HOA} was also observed ($R^2 = 0.85$).

Evolution of Organic Markers during the NPF Events

The two important ions, m/z 44 (CO_2^+) and m/z 43 (mostly $C_2H_3O^+$), can characterize the evolution of OA in the atmosphere (Ng *et al.*, 2010). The ratio of fractions f_{44} to f_{43} provides a measure of how the chemical functionality of the ambient OA evolves with oxidation (i.e., degree of oxidation). Higher f_{44} has been associated to less volatile, highly oxidized OA (LV-OOA) and lower f_{44} has been associated to semi-volatile, less oxidized OA (SV-OOA) (Ulbrich *et al.*, 2009) so with aging f_{44}/f_{43} ratio tends to increase significantly. In Fig. S5, we have plotted diurnal variation of fractions f_{43} , f_{44} and the ratio of f_{44} to f_{43} . An increase in f_{44} and f_{44}/f_{43} and concurrent decrease in f_{43} during the NPF event days suggest that significant fraction of the total OA mass might have consisted of less volatile, highly oxidized OA. However, on the 5 April NPF event, f_{44}/f_{43} at very high aerosol loading agrees with the observed dominance of HOA during this day.

A continuous flow-chamber experiment showed the maximum variability in chemical composition of aerosols for low OA loadings ($< 15 \mu\text{g m}^{-3}$) compared to high loadings (Shilling *et al.*, 2009). Furthermore, Ng *et al.* (2010, 2011) showed that freshly oxidized OAs (SV-OOA) occupy the lower right part of the triangular region of the f_{43} versus f_{44} plot, while the more oxidized and subsequently more aged OA (LV-OOA) occupies upper left part of the triangle. Therefore, we have plotted f_{43} versus f_{44} for 10:00–18:00 local time on all observation days in Fig. 4(b). The ambient OA components fall inside the triangular space proposed by Ng *et al.* (2010). The data before 10:00 and after 18:00 local time excluded deliberately in Fig. 4(b) to minimize the direct influence of morning and evening traffic hours, respectively and also, newly formed particles on NPF event days unlikely to generate sufficient signal at lowest detectable size by the AMS (i.e., diameter of 40 nm) before 10:00 local time. Overall, OAs appeared to be concentrated in the upper half of the triangular region suggesting more oxidized and/or aged OAs, except on 5 April. On this day, the OAs were concentrated in the lower left half of the triangular region, suggesting the occurrence of primary and less oxidized OAs

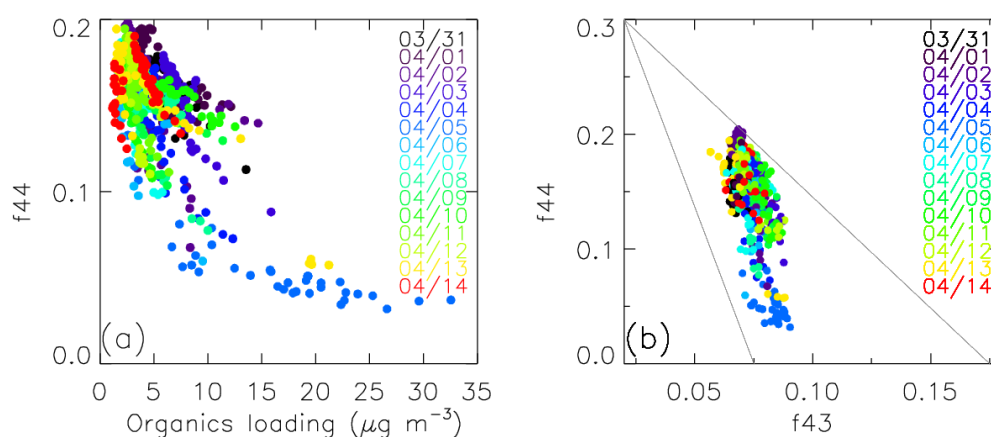


Fig. 4. (a) Scatter plot of f44 and organics loading and (b) scatter plot of f44 vs. f43, for 10:00–18:00 local time. The triangle from Ng *et al.* (2010) is drawn in (b) as a visual aid (grey lines). Each data point is 10 minute average.

(Figs. 3 and S5). To further substantiate the source of primary OAs on 5 April, f43 versus f44 re-plotted as a function of f57 (Fig. S6). It can be seen that the primary emitted OAs with higher f57 lies in the lower left part of the triangular region on 5 April, indicative of the possible source of combustion-generated primary OAs. Salimi *et al.* (2015) also showed that the particles originated from vehicular emissions cluster at the lower left corner of the triangular region, whereas particles originated from natural nucleation events cluster somewhere at the top of the triangle. This further suggests that the 5 April NPF event might have encountered large concentrations of ultrafine particles of primary source, particularly after 12:30 local time. A recent study also highlighted that NPF is not inevitably the major source of large number concentrations of ultrafine particles to the atmosphere, and that the large concentrations of ultrafine particles are direct result of traffic emissions in urban areas (Rönkkö *et al.*, 2017).

Evidence of Nitrogen-containing Organic Compounds in Sub-micron Aerosols

To infer the role of nitrogen-containing compounds during NPF and non-NPF events, the mass concentration of nitrogen-containing fragments ($C_xH_yN^+$), m/z 86 ion ($C_5H_{12}N^+$) and m/z 18 ion (NH_4^+) are plotted in Fig. 5. The morning and evening hour enhancements in $C_xH_yN^+$ and $C_5H_{12}N^+$ coincides with the traffic rush hours, analogous to the diurnal pattern observed for f57 and HOA (Fig. 3). Significant enhancement of $C_xH_yN^+$ in sub-micron particles during NPF events suggests that this class of compounds could play an important role in aerosol formation and growth processes. A recent study also indicated the likely presence of alkyl amines in sub-micron aerosols during the NPF events in a mixed-urban-biogenic environment, with significant enhancements in nitrogen-containing organic ions (Setyan *et al.*, 2014). Furthermore, the concurrent increase in ammonium in sub-micron particles (Fig. 5) plausibly suggests that ammonium together with sulfate involved in the initial growth of ultrafine particles, forming ammonium sulfate and ammonium bisulfate. Although, the previous studies have expressed the significance of aminium salt formation

in ambient aerosols (Pratt *et al.*, 2009; Smith *et al.*, 2010) via displacing ammonium with aminium species in secondary organic aerosol (Murphy *et al.*, 2007), and such exchange of ammonium in sub-micron aerosols by aminium salt is expected to occur within a few hours (Lloyd *et al.*, 2009). A significant enhancement of $C_xH_yN^+$ on the 5 April NPF event day suggests that such chemical transformation within sub-micron aerosols is possible. At urban sites, gas-phase ammonia concentrations range from sub-ppbv to tens-of-ppbv level, whereas amines concentrations are typically found in the range of pptv to tens of pptv (Hanson *et al.*, 2011; Dawson *et al.*, 2014; You *et al.*, 2014). Considering a higher ambient concentration and large uptake coefficient for ammonia than those for amines (Wang *et al.*, 2010), it is plausible that sulfate acidic particles will be dominantly neutralized by ammonia. But, recent laboratory experiments by Liggio *et al.* (2011) indicated that the reactive uptake coefficient for uptake of ammonia by acidic sulfate aerosols decreases with increasing OA mass and it is possible that the heterogeneous reaction of alkyl amines leads to the efficient growth of more acidic particles during the NPF event (Wang *et al.*, 2010).

Furthermore, we have calculated averaged mass spectra of $C_xH_yN^+$ and $C_xH_yNO_z^+$ fragments to examine the chemical composition of sub-micron aerosols for the Type-I, Type-II NPF and Type-IV non-NPF event days (Fig. 6). Quantitative analysis of the aerosol chemical composition showed that generally, amine family ($C_xH_yN^+$) ions were present in sub-micron aerosols during Type-I and Type-II NPF events, with significantly enhanced signal intensity of amine family ions during Type-I NPF events (Fig. 6(a)). For instance, significantly enhanced signal intensity for amine families such m/z 30 CH_4N^+ and m/z 42 $C_2H_4N^+$ can be seen, with about more than twofold signal intensity on 5 April compared to that of other Type-I or Type-II NPF event days. We observed increased signals for other noticeable amine fragments too (i.e., m/z 58 $C_3H_8N^+$, m/z 70 $C_4H_8N^+$, and m/z 86 $C_5H_{12}N^+$) on Type-I NPF event days as compared to non-NPF event days. While these fragments in ambient aerosols are shown to be expected from trimethylamine (Silva *et al.*, 2008), secondary organic aerosol chamber experiment

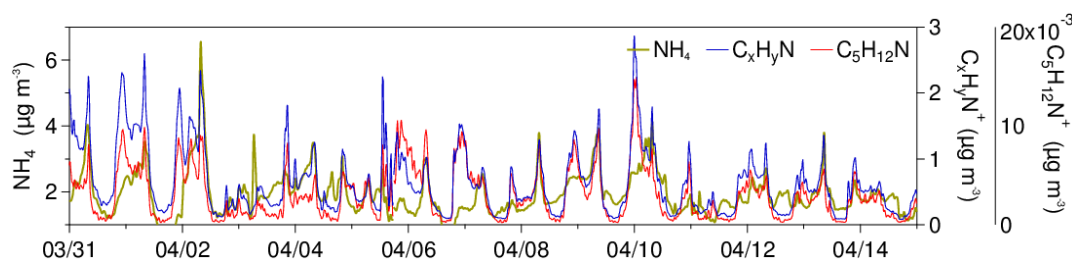


Fig. 5. Diurnal variation of mass concentrations of nitrogen-containing fragments ($C_xH_yN^+$), m/z 86 ion ($C_5H_{12}N^+$) and m/z 18 ion (NH_4^+) on observed non-NPF (marked by red rectangle) and NPF (blue rectangle) event days.

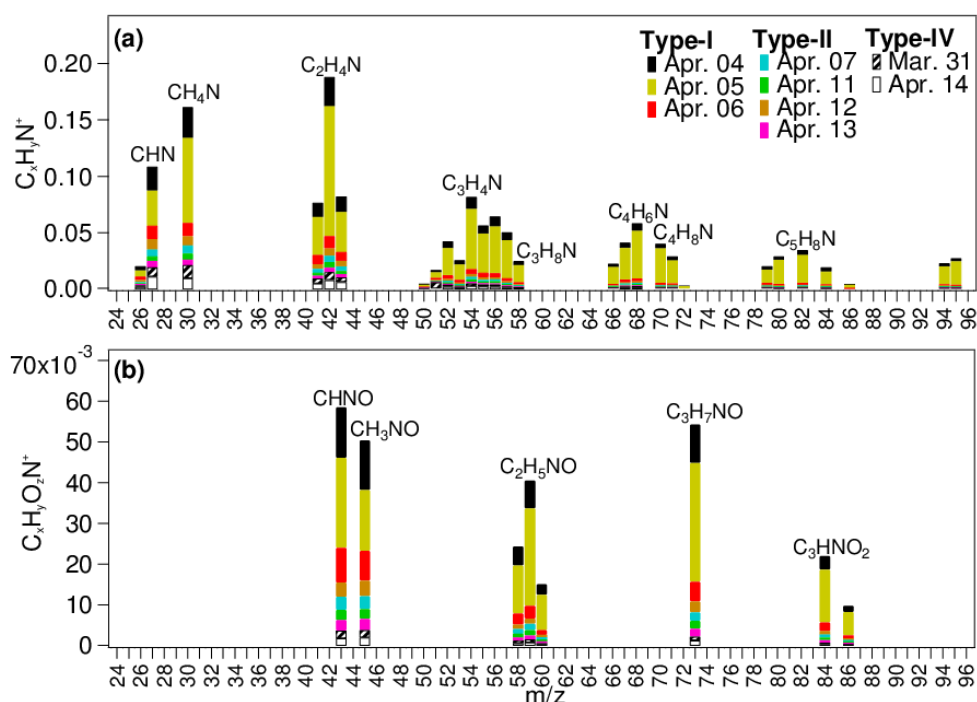


Fig. 6. Averaged mass spectra of (a) $C_xH_yN^+$ and (b) $C_xH_yO_zN^+$ fragments for time period 12:00–18:00 local time on Type-I (strong), Type-II (moderate to weak) and Type-IV (non-NPF) events.

revealed that it is a combined signal from nitrate, and fragment of amines and amino acids (Murphy *et al.*, 2007). The mass spectra listed by the NIST chemistry web book also show a strong peak at m/z 30 for higher alkylamines. The average mass spectra also showed small enhancements at m/z 55, 67 and 79 ($C_xH_5N^+$ ions) indicative of nitrile- and/or pyridine-type fragments. Since biomass-burning- and/or residential-cooking-generated organic aerosols were not evident at our site, perhaps traffic emissions could be the source of these compounds, especially on 5 April, which thought to be under the influence of traffic plume. $C_xH_yO_zN^+$ families (i.e., m/z 59, C_2H_5NO and m/z 72, C_3H_7NO) also showed enhanced signal intensity, especially on 5 April (Fig. 6(b)) as compared to Type-II NPF and Type-IV non-NPF event days.

CONCLUSIONS

We conducted simultaneous measurements via SMPS (TSI Inc.) and HR-ToF-AMS (Aerodyne) to investigate the

chemical properties of sub-micron aerosols during new particle formation (NPF) events at a highly polluted urban site, Kanpur, on the Indo-Gangetic Plain in India. The particle number-size distributions showed that regional NPF events occurred very frequently (on the observation days) in Kanpur under conditions with relatively high aerosol loading. During these events, the particle growth rate varied from 2.7 to 6.7 $nm\ h^{-1}$. As the AMS can not detect particles smaller than 40 nm in diameter, our study was not intended to address the chemistry driving the NPF. Our analysis of the AMS-measured organic mass spectra indicated that oxygenated organic aerosols, including hydrocarbon-like organic aerosol (HOA) and biomass burning organic aerosol (BBOA), which formed the largest and the second largest fraction, respectively, constituted approximately 75% of the total sub-micron aerosol mass on NPF event days. The BBOA tracers m/z 60 and m/z 73 showed typical diurnal patterns with enhanced signal intensity during peak traffic hours, whereas the HOA tracer m/z 57 displayed substantially elevated intensity during all of the NPF event days.

Furthermore, we examined the evolution of organic markers, such as m/z 44 and m/z 43, on the event days. The increase in the m/z 43 fraction (f43) and the decreases in the m/z 44 fraction (f44) and the f44/f43 ratio suggest that the growth of new particles is likely driven by the condensation of less volatile and highly oxidized organic compounds. As a result, a rapidly decreasing f44 along with an increasing OA mass load during NPF event days was observed. However, an NPF event on 5 April exhibited both a noontime decrease in f44 and an increase in the f44/f43 ratio, indicating the presence of semi-volatile, less oxidized—and therefore primary—organic species in the total OA mass. This difference is illustrated by a scatter plot depicting f43 versus f44; the OA fractions on 5 April populate the lower left corner of a triangular region, unlike the fractions from the rest of the observation period, which are concentrated in the upper half of this region. In general, though, nitrogen-containing organic ions (viz., CHN^+ , CH_4N^+ , $\text{C}_2\text{H}_4\text{N}^+$, $\text{C}_3\text{H}_8\text{N}^+$, and $\text{C}_5\text{H}_{12}\text{N}^+$) dominate the composition of sub-micron aerosols during NPF, which demonstrates the critical role of amine fragments in this process.

In spite of high concentrations of pre-existing aerosols, observations in urban environments confirm the frequent occurrence of NPF, which must be considered when quantifying its effects on the climate, especially in cities. To identify the species that contribute to particle formation and growth, the chemistry and dynamics of atmospheric ultrafine particles must be evaluated by conducting direct measurements using state-of-the-art instrumentation techniques for ultrafine particles.

ACKNOWLEDGMENTS

We acknowledge the support of IIT Kanpur for providing HR-ToF-AMS for PG research and teaching. VPK would like to thank University Grants Commission, Government of India, for Start-Up Grant [Ref. No. F.4-5(230-FRP/2015/BSR)] and DST-SERB for early Career Research Award (ECR/2016/001333). HY thank the support from the National Key Research and Development Program of China (Grant No. 2016YFC0203100). Authors acknowledge the financial support given by the Earth System Science Organization, Ministry of Earth Sciences, Government of India (Grant No. MM/NERC-MoES-03/2014/002), to conduct this research under Monsoon Mission. Authors are thankful to anonymous reviewers for their constructive suggestions to improve the quality of the manuscript.

SUPPLEMENTARY MATERIAL

Supplementary data associated with this article can be found in the online version at <http://www.aaqr.org>.

REFERENCES

- Aiken, A.C., Salcedo, D., Cubison, M.J., Huffman, J.A., DeCarlo, P.F., Ulbrich, I.M., Docherty, K.S., Sueper, D., Kimmel, J.R., Worsnop, D.R., Trimborn, A., Northway, M., Stone, E.A., Schauer, J.J., Volkamer, R.M., Fortner, E., de Foy, B., Wang, J., Laskin, A., ... Jimenez, J.L. (2009). Mexico City aerosol analysis during MILAGRO using high resolution aerosol mass spectrometry at the urban supersite (T0) – Part 1: Fine particle composition and organic source apportionment. *Atmos. Chem. Phys.* 9: 6633–6653.
- Almeida, J., Schobesberger, S., Kurten, A., Ortega, I.K., Kupiainen-Maatta, O., Praplan, A.P., Adamov, A., Amorim, A., Bianchi, F., Breitenlechner, M., David, A., Dommen, J., Donahue, N.M., Downard, A., Dunne, E., Duplissy, J., Ehrhart, S., Flagan, R.C., Franchin, A., ... Kirkby, J. (2013). Molecular understanding of sulphuric acid-amine particle nucleation in the atmosphere. *Nature*. 502: 359–363.
- Andreae, M.O. and Rosenfeld, D. (2008). Aerosol–cloud–precipitation interactions. Part 1. The nature and sources of cloud-active aerosols. *Earth Sci. Rev.* 89: 13–41.
- Babu, S.S., Kompalli, S.K. and Moorthy, K.K. (2016). Aerosol number size distributions over a coastal semi urban location: Seasonal changes and ultrafine particle bursts. *Sci. Total Environ.* 563–564: 351–365.
- Bzdek, B.R., Ridge, D.P. and Johnston, M.V. (2011). Amine Reactivity with Charged Sulfuric Acid Clusters. *Atmos. Chem. Phys.* 11: 8735–8743.
- Bzdek, B.R., Zordan, C.A., Pennington, M.R., Luther, G.W. and Johnston, M.V. (2012). Quantitative Assessment of the Sulfuric Acid Contribution to New Particle Growth. *Environ. Sci. Technol.* 46: 4365–4373.
- Canagaratna, M.R., Jayne, J.T., Jimenez, J.L., Allan, J.D., Alfarra, M.R., Zhang, Q., Onasch, T.B., Drewnick, F., Coe, H., Middlebrook, A., Delia, A., Williams, L.R., Trimborn, A.M., Northway, M.J., DeCarlo, P.F., Kolb, C.E., Davidovits, P. and Worsnop, D.R. (2007). Chemical and microphysical characterization of ambient aerosols with the aerodyne aerosol mass spectrometer. *Mass Spectrom. Rev.* 26: 185–222.
- Canagaratna, M.R., Onasch, T.B., Wood, E.C., Herndon, S.C., Jayne, J.T., Cross, E.S., Miake-Lye, R.C., Kolb, C.E. and Worsnop, D.R. (2010). Evolution of vehicle exhaust particles in the atmosphere. *J. Air Waste Manage. Assoc.* 60: 1192–1203.
- Canagaratna, M.R., Jimenez, J.L., Kroll, J.H., Chen, Q., Kessler, S.H., Massoli, P., Hildebrandt Ruiz, L., Fortner, E., Williams, L.R., Wilson, K.R., Surratt, J.D., Donahue, N.M., Jayne, J.T. and Worsnop, D.R. (2015). Elemental ratio measurements of organic compounds using aerosol mass spectrometry: Characterization, improved calibration, and implications. *Atmos. Chem. Phys.* 15: 253–272.
- Chakraborty, A., Bhattu, D., Gupta, T., Tripathi, S.N. and Canagaratna, M.R. (2015). Real-time measurements of ambient aerosols in a polluted Indian city: Sources, characteristics, and processing of organic aerosols during foggy and nonfoggy periods. *J. Geophys. Res.* 120: 9006–9019.
- Creamean, J.M., Ault, A.P., Ten Hoeve, J.E., Jacobson, M.Z., Roberts, G.C. and Prather, K.A. (2011). Measurements of aerosol chemistry during new particle formation events at a remote rural mountain site. *Environ. Sci. Technol.* 45: 8208–8216.

- Dal Maso, M., Kulmala, M., Riipinen, I., Wagner, R., Hussein, T., Aalto, P.P. and Lehtinen, K.E.J. (2005). Formation and growth of fresh atmospheric aerosols: Eight years of aerosol size distribution data from SMEAR II, Hyytiälä, Finland. *Boreal Env. Res.* 10: 323–336.
- Dawson, M.L., Varner, M.E., Perraud, V., Ezell, M.J., Gerber, R.B. and Finlayson-Pitts, B.J. (2012). Simplified mechanism for new particle formation from methanesulfonic acid, amines, and water via experiments and ab initio calculations. *Proc. Natl. Acad. Sci. U.S.A.* 109: 18719–18724.
- Dawson, M.L., Perraud, V., Gomez, A., Arquero, K.D., Ezell, M.J. and Finlayson-Pitts, B.J. (2014). Measurement of gas-phase ammonia and amines in air by collection onto an ion exchange resin and analysis by ion chromatography. *Atmos. Meas. Tech.* 7: 2733–2744.
- DeCarlo, P.F., Kimmel, J.R., Trimborn, A., Northway, M.J., Jayne, J.T., Aiken, A.C., Gonin, M., Fuhrer, K., Horvath, T., Docherty, K.S., Worsnop, D.R. and Jimenez, J.L. (2006). Field-deployable, high-resolution, time-of-flight aerosol mass spectrometer. *Anal. Chem.* 78: 8281–8289.
- Erupe, M.E., Viggiano, A.A. and Lee, S.H. (2011). The effect of trimethylamine on atmospheric nucleation involving H₂SO₄. *Atmos. Chem. Phys.* 11: 4767–4775.
- Facchini, M.C., Decesari, S., Rinaldi, M., Carbone, C., Finessi, E., Mircea, M., Fuzzi, S., Moretti, F., Tagliavini, E., Ceburnis, D. and O'Dowd, C.D. (2008). Important source of marine secondary organic aerosol from biogenic amines. *Environ. Sci. Technol.* 42: 9116–9121.
- Gaur, A., Tripathi, S.N., Kanawade, V.P., Tare, V. and Shukla, S.P. (2014). Four-year measurements of trace gases (SO₂, NO_x, CO, and O₃) at an urban location, Kanpur, in Northern India. *J. Atmos. Chemis.* 71: 283–301.
- Hanson, D.R., McMurry, P.H., Jiang, J., Tanner, D. and Huey, L.G. (2011). Ambient pressure proton transfer mass spectrometry: Detection of amines and ammonia. *Environ. Sci. Technol.* 45: 8881–8888.
- Hussein, T., Puustinen, A., Aalto, P.P., Mäkelä, J.M., Hämeri, K. and Kulmala, M. (2004). Urban aerosol number size distributions. *Atmos. Chem. Phys.* 4: 391–411.
- Hyytiäinen, A.P., Lihavainen, H., Komppula, M., Panwar, T.S., Sharma, V.P., Hooda, R.K. and Viisanen, Y. (2010). Aerosol measurements at the Gual Pahari EUCAARI station: Preliminary results from in-situ measurements. *Atmos. Chem. Phys.* 10: 7241–7252.
- Jen, C.N., McMurry, P.H. and Hanson, D.R. (2014). Stabilization of sulfuric acid dimers by ammonia, methylamine, dimethylamine, and trimethylamine. *J. Geophys. Res.* 119: 7502–7514.
- Jimenez, J.L., Jayne, J.T., Shi, Q., Kolb, C.E., Worsnop, D.R., Yourshaw, I., Seinfeld, J.H., Flagan, R.C., Zhang, X., Smith, K.A., Morris, J.W. and Davidovits, P. (2003). Ambient aerosol sampling using the Aerodyne Aerosol Mass Spectrometer. *J. Geophys. Res.* 108: 8425.
- Kamra, A.K., Siingh, D., Gautam, A.S., Kanawade, V.P., Tripathi, S.N. and Srivastava, A.K. (2015). Atmospheric ions and new particle formation events at a tropical location, Pune, India. *Q. J. R. Meteorolog. Soc.* 141: 3140–3156.
- Kanawade, V.P., Benson, D.R. and Lee, S.H. (2012). Statistical analysis of 4-year observations of aerosol sizes in a semi-rural continental environment. *Atmos. Environ.* 59: 30–38.
- Kanawade, V.P., Shika, S., Pöhlker, C., Rose, D., Suman, M.N.S., Gadhavi, H., Kumar, A., Nagendra, S.M.S., Ravikrishna, R., Yu, H., Sahu, L.K., Jayaraman, A., Andreae, M.O., Pöschl, U. and Gunthe, S.S. (2014a). Infrequent occurrence of new particle formation at a semi-rural location, Gadanki, in tropical Southern India. *Atmos. Environ.* 94: 264–273.
- Kanawade, V.P., Tripathi, S.N., Bhattu, D. and Shamjad, P.M. (2014b). Sub-micron particle number size distributions characteristics at an urban location, Kanpur, in the Indo-Gangetic Plain. *Atmos. Res.* 147–148: 121–132.
- Kanawade, V.P., Tripathi, S.N., Siingh, D., Gautam, A.S., Srivastava, A.K., Kamra, A.K., Soni, V.K. and Sethi, V. (2014c). Observations of new particle formation at two distinct Indian subcontinental urban locations. *Atmos. Environ.* 96: 370–379.
- Kirkby, J., Curtius, J., Almeida, J., Dunne, E., Duplissy, J., Ehrhart, S., Franchin, A., Gagne, S., Ickes, L., Kurten, A., Kupc, A., Metzger, A., Riccobono, F., Rondo, L., Schobesberger, S., Tsagkogeorgas, G., Wimmer, D., Amorim, A., Bianchi, F., ... Kulmala, M. (2011). Role of sulphuric acid, ammonia and galactic cosmic rays in atmospheric aerosol nucleation. *Nature.* 476: 429–433.
- Kulmala, M., Maso, M.D., Mäkelä, J.M., Pirjola, L., Väkevä, M., Aalto, P., Miikkulainen, P., Hämeri, K., and O'Dowd, C.D. (2001). On the formation, growth and composition of nucleation mode particles. *Tellus B* 53: 479–490.
- Kulmala, M., Vehkamäki, H., Petäjä, T., Dal Maso, M., Lauri, A., Kerminen, V.M., Birmili, W. and McMurry, P.H. (2004). Formation and growth rates of ultrafine atmospheric particles: A review of observations. *J. Aerosol Sci.* 35: 143–176.
- Kulmala, M., Kontkanen, J., Junninen, H., Lehtipalo, K., Manninen, H.E., Nieminen, T., Petäjä, T., Sipilä, M., Schobesberger, S., Rantala, P., Franchin, A., Jokinen, T., Järvinen, E., Äijälä, M., Kangasluoma, J., Hakala, J., Aalto, P.P., Paasonen, P., Mikkilä, J., ... Worsnop, D.R. (2013). Direct observations of atmospheric aerosol nucleation. *Science* 339: 943–946.
- Kürten, A., Jokinen, T., Simon, M., Sipilä, M., Sarnela, N., Junninen, H., Adamov, A., Almeida, J., Amorim, A., Bianchi, F., Breitenlechner, M., Dommen, J., Donahue, N.M., Duplissy, J., Ehrhart, S., Flagan, R.C., Franchin, A., Hakala, J., Hansel, A., ... Curtius, J. (2014). Neutral molecular cluster formation of sulfuric acid–dimethylamine observed in real time under atmospheric conditions. *Proc. Natl. Acad. Sci. U.S.A.* 111: 15019–15024.
- Kurtén, T., Loukonen, V., Vehkamäki, H. and Kulmala, M. (2008). Amines are likely to enhance neutral and ion-induced sulfuric acid–water nucleation in the atmosphere more effectively than ammonia. *Atmos. Chem. Phys.* 8: 4095–4103.

- Leena, P.P., Anil Kumar, V., Dani, K.K., Sombawne, S.M., Murugavel, P. and Pandithurai, G. (2017). Evidence of new particle formation during post monsoon season over a high-altitude site of the Western Ghats, India. *Toxicol. Environ. Chem.* 99: 652–664.
- Liggio, J., Li, S.M., Vlasenko, A., Stroud, C. and Makar, P. (2011). Depression of ammonia uptake to sulfuric acid aerosols by competing uptake of ambient organic gases. *Environ. Sci. Technol.* 45: 2790–2796.
- Lloyd, J.A., Heaton, K.J. and Johnston, M.V. (2009). Reactive uptake of trimethylamine into ammonium nitrate particles. *Phys. Chem. A* 113: 4840–4843.
- Mäkelä, J.M., Yli-Koivisto, S., Hiltunen, V., Seidl, W., Swietlicki, E., Teinilä, K., Sillanpää, M., Koponen, I.K., Paatero, J., Rosman, K. and Hämeri, K. (2003). Chemical composition of aerosol during particle formation events in boreal forest. *Tellus B* 53: 380–393.
- Mönkkönen, P., Koponen, I.K., Lehtinen, K.E.J., Hämeri, K., Uma, R. and Kulmala, M. (2005). Measurements in a highly polluted Asian mega city: observations of aerosol number size distribution, modal parameters and nucleation events. *Atmos. Chem. Phys.* 5: 57–66.
- Moorthy, K.K., Sreekanth, V., Prakash Chaubey, J., Gogoi, M.M., Suresh Babu, S., Kumar Kompalli, S., Bagare, S.P., Bhatt, B.C., Gaur, V.K., Prabhu, T.P. and Singh, N.S. (2011). Fine and ultrafine particles at a near-free tropospheric environment over the high-altitude station Hanle in the Trans-Himalaya: New particle formation and size distribution. *J Geophys. Res.* 116: D20212.
- Murphy, S.M., Sorooshian, A., Kroll, J.H., Ng, N.L., Chhabra, P., Tong, C., Surratt, J.D., Knipping, E., Flagan, R.C. and Seinfeld, J.H. (2007). Secondary aerosol formation from atmospheric reactions of aliphatic amines. *Atmos. Chem. Phys.* 7: 2313–2337.
- Neitola, K., Asmi, E., Komppula, M., Hyvärinen, A.P., Raatikainen, T., Panwar, T.S., Sharma, V.P. and Lihavainen, H. (2011). New particle formation infrequently observed in Himalayan foothills – why? *Atmos. Chem. Phys.* 11: 8447–8458.
- Németh, Z., Rosati, B., Zíková, N., Salma, I., Bozó, L., Dameto de España, C., Schwarz, J., Ždímal, V. and Wonaschütz, A. (2018). Comparison of atmospheric new particle formation events in three Central European cities. *Atmos. Environ.* 178: 191–197.
- Ng, N.L., Canagaratna, M.R., Zhang, Q., Jimenez, J.L., Tian, J., Ulbrich, I.M., Kroll, J.H., Docherty, K.S., Chhabra, P.S., Bahreini, R., Murphy, S.M., Seinfeld, J.H., Hildebrandt, L., Donahue, N.M., DeCarlo, P.F., Lanz, V.A., Prévôt, A.S.H., Dinar, E., Rudich, Y. and Worsnop, D.R. (2010). Organic aerosol components observed in Northern Hemispheric datasets from Aerosol Mass Spectrometry. *Atmos. Chem. Phys.* 10: 4625–4641.
- Ng, N.L., Canagaratna, M.R., Jimenez, J.L., Chhabra, P.S., Seinfeld, J.H. and Worsnop, D.R. (2011). Changes in organic aerosol composition with aging inferred from aerosol mass spectra. *Atmos. Chem. Phys.* 11: 6465–6474.
- Pierce, J.R. and Adams, P.J. (2009). Uncertainty in global CCN concentrations from uncertain aerosol nucleation and primary emission rates. *Atmos. Chem. Phys.* 9: 1339–1356.
- Pratt, K.A., Hatch, L.E. and Prather, K.A. (2009). Seasonal volatility dependence of ambient particle phase amines. *Environ. Sci. Technol.* 43: 5276–5281.
- Prenni, A.J., DeMott, P.J., Kreidenweis, S.M., Sherman, D.E., Russell, L.M. and Ming, Y. (2001). The effects of low molecular weight dicarboxylic acids on cloud formation. *J. Phys. Chem. A* 105: 11240–11248.
- Rönkkö, T., Kuuluvainen, H., Karjalainen, P., Keskinen, J., Hillamo, R., Niemi, J.V., Pirjola, L., Timonen, H.J., Saarikoski, S., Saukko, E., Järvinen, A., Silvennoinen, H., Rostedt, A., Olin, M., Yli-Ojanperä, J., Nousiainen, P., Kousa, A. and Dal Maso, M. (2017). Traffic is a major source of atmospheric nanocluster aerosol. *Proc. Natl. Acad. Sci. U.S.A.* 114: 7549–7554.
- Salimi, F., Crilley, L.R., Stevanovic, S., Ristovski, Z., Mazaheri, M., He, C., Johnson, G., Ayoko, G. and Morawska, L. (2015). Insights into the growth of newly formed particles in a subtropical urban environment. *Atmos. Chem. Phys.* 15: 13475–13485.
- Samoli, E., Andersen, Z.J., Katsouyanni, K., Hennig, F., Kuhlbusch, T.A.J., Bellander, T., Cattani, G., Cyrus, J., Forastiere, F., Jacquemin, B., Kulmala, M., Lanki, T., Loft, S., Massling, A., Tobias, A. and Stafoggia, M. (2016). Exposure to ultrafine particles and respiratory hospitalisations in five European cities. *Eur. Respir. J.* 48: 674–682.
- Sarangi, C., Tripathi, S.N., Kanawade, V.P., Koren, I. and Pai, D.S. (2017). Investigation of the aerosol–cloud–rainfall association over the Indian summer monsoon region. *Atmos. Chem. Phys.* 17: 5185–5204.
- Sarangi, C., Kanawade, V.P., Tripathi, S.N., Thomas, A. and Ganguly, D. (2018). Aerosol-induced intensification of cooling effect of clouds during Indian summer monsoon. *Nat. Commun.* 9: 3754.
- Schobesberger, S., Junninen, H., Bianchi, F., Lönn, G., Ehn, M., Lehtipalo, K., Dommen, J., Ehrhart, S., Ortega, I.K., Franchin, A., Nieminen, T., Riccobono, F., Hutterli, M., Duplissy, J., Almeida, J., Amorim, A., Breitenlechner, M., Downard, A.J., Dunne, E.M., ... Worsnop, D.R. (2013). Molecular understanding of atmospheric particle formation from sulfuric acid and large oxidized organic molecules. *Proc. Natl. Acad. Sci. U.S.A.* 110: 17223–17228.
- Seigneur, C. (2009). Current understanding of ultrafine particulate matter emitted from mobile sources. *J. Air Waste Manage. Assoc.* 59: 3–17.
- Setyan, A., Song, C., Merkel, M., Knighton, W.B., Onasch, T.B., Canagaratna, M.R., Worsnop, D.R., Wiedensohler, A., Shilling, J.E. and Zhang, Q. (2014). Chemistry of new particle growth in mixed urban and biogenic emissions – insights from CARES. *Atmos. Chem. Phys.* 14: 6477–6494.
- Shen, X.J., Sun, J.Y., Zhang, Y.M., Wehner, B., Nowak, A., Tuch, T., Zhang, X.C., Wang, T.T., Zhou, H.G., Zhang, X.L., Dong, F., Birmili, W. and Wiedensohler, A. (2011). First long-term study of particle number size distributions and new particle formation events of regional aerosol in

- the North China Plain. *Atmos. Chem. Phys.* 11: 1565–1580.
- Shilling, J.E., Chen, Q., King, S.M., Rosenoern, T., Kroll, J.H., Worsnop, D.R., DeCarlo, P.F., Aiken, A.C., Sueper, D., Jimenez, J.L. and Martin, S.T. (2009). Loading-dependent elemental composition of α -pinene SOA particles. *Atmos. Chem. Phys.* 9: 771–782.
- Siingh, D., Gautam, A.S., Kamra, A.K. and Komsaare, K. (2013). Nucleation events for the formation of charged aerosol particles at a tropical station — Preliminary results. *Atmos. Res.* 132–133: 239–252.
- Silva, P.J., Erupe, M.E., Price, D., Elias, J., G.J., Malloy, Q., Li, Q., Warren, B. and Cocker, D.R. (2008). Trimethylamine as precursor to secondary organic aerosol formation via nitrate radical reaction in the atmosphere. *Environ. Sci. Technol.* 42: 4689–4696.
- Smith, J.N., Barsanti, K.C., Friedli, H.R., Ehn, M., Kulmala, M., Collins, D.R., Scheckman, J.H., Williams, B.J. and McMurry, P.H. (2010). Observations of aminium salts in atmospheric nanoparticles and possible climatic implications. *Proc. Natl. Acad. Sci. U.S.A.* 107: 6634–6639.
- Sobhan Kumar, K., Suresh Babu, S., Krishna Moorthy, K., Mukunda, M.G., Vijayakumar, S.N. and Jai Prakash, C. (2014). The formation and growth of ultrafine particles in two contrasting environments: A case study. *Ann. Geophys.* 32: 817–830.
- Sorooshian, A., Ng, N.L., Chan, A.W.H., Feingold, G., Flagan, R.C. and Seinfeld, J.H. (2007). Particulate organic acids and overall water-soluble aerosol composition measurements from the 2006 Gulf of Mexico Atmospheric Composition and Climate Study (GoMACCS). *J. Geophys. Res.* 112: D13201.
- Sorooshian, A., Murphy, S.M., Hersey, S., Gates, H., Padro, L.T., Nenes, A., Brechtel, F.J., Jonsson, H., Flagan, R.C. and Seinfeld, J.H. (2008). Comprehensive airborne characterization of aerosol from a major bovine source. *Atmos. Chem. Phys.* 8: 5489–5520.
- Spracklen, D.V., Carslaw, K.S., Kulmala, M., Kerminen, V.M., Mann, G.W. and Sihto, S.L. (2006). The contribution of boundary layer nucleation events to total particle concentrations on regional and global scales. *Atmos. Chem. Phys.* 6: 5631–5648.
- Spracklen, D.V., Carslaw, K.S., Kulmala, M., Kerminen, V.M., Sihto, S.L., Riipinen, I., Merikanto, J., Mann, G.W., Chipperfield, M.P., Wiedensohler, A., Birmili, W. and Lihavainen, H. (2008). Contribution of particle formation to global cloud condensation nuclei concentrations. *Geophys. Res. Lett.* 35: L06808.
- Stanier, C.O., Khlystov, A.Y. and Pandis, S.N. (2004). Ambient aerosol size distributions and number concentrations measured during the Pittsburgh Air Quality Study (PAQS). *Atmos. Environ.* 38: 3275–3284.
- Tao, Y., Ye, X., Jiang, S., Yang, X., Chen, J., Xie, Y. and Wang, R. (2016). Effects of amines on particle growth observed in new particle formation events. *J. Geophys. Res.* 121: 324–335.
- Ulbrich, I.M., Canagaratna, M.R., Zhang, Q., Worsnop, D.R. and Jimenez, J.L. (2009). Interpretation of organic components from Positive Matrix Factorization of aerosol mass spectrometric data. *Atmos. Chem. Phys.* 9: 2891–2918.
- Wang, L., Khalizov, A.F., Zheng, J., Xu, W., Ma, Y., Lal, V. and Zhang, R. (2010). Atmospheric nanoparticles formed from heterogeneous reactions of organics. *Nat. Geosci.* 3: 238–242.
- Wehner, B. and Wiedensohler, A. (2003). Long term measurements of submicrometer urban aerosols: Statistical analysis for correlations with meteorological conditions and trace gases. *Atmos. Chem. Phys.* 3: 867–879.
- Wu, Z., Hu, M., Lin, P., Liu, S., Wehner, B. and Wiedensohler, A. (2008). Particle number size distribution in the urban atmosphere of Beijing, China. *Atmos. Environ.* 42: 7967–7980.
- Yao, L., Garmash, O., Bianchi, F., Zheng, J., Yan, C., Kontkanen, J., Junninen, H., Mazon, S.B., Ehn, M., Paasonen, P., Sipilä, M., Wang, M., Wang, X., Xiao, S., Chen, H., Lu, Y., Zhang, B., Wang, D., Fu, Q., ... Wang, L. (2018). Atmospheric new particle formation from sulfuric acid and amines in a Chinese megacity. *Science* 361: 278–281.
- You, Y., Kanawade, V.P., de Gouw, J.A., Guenther, A.B., Madronich, S., Sierra-Hernández, M.R., Lawler, M., Smith, J.N., Takahama, S., Ruggeri, G., Koss, A., Olson, K., Baumann, K., Weber, R.J., Nenes, A., Guo, H., Edgerton, E.S., Porcelli, L., Brune, W.H., Goldstein, A.H. and Lee, S.H. (2014). Atmospheric amines and ammonia measured with a chemical ionization mass spectrometer (CIMS). *Atmos. Chem. Phys.* 14: 12181–12194.
- Yu, F. and Luo, G. (2014). Modeling of gaseous methylamines in the global atmosphere: Impacts of oxidation and aerosol uptake. *Atmos. Chem. Phys.* 14: 12455–12464.
- Yu, H., McGraw, R. and Lee, S.H. (2012). Effects of amines on formation of sub-3 nm particles and their subsequent growth. *Geophys. Res. Lett.* 39: L02807.
- Yu, H., Ren, L. and Kanawade, V.P. (2017). New particle formation and growth mechanisms in highly polluted environments. *Curr. Pollut. Rep.* 3: 245–253.
- Zhang, Q., Alfarra, M.R., Worsnop, D.R., Allan, J.D., Coe, H., Canagaratna, M.R. and Jimenez, J.L. (2005). Deconvolution and quantification of hydrocarbon-like and oxygenated organic aerosols based on aerosol mass spectrometry. *Environ. Sci. Technol.* 39: 4938–4952.
- Zhang, Q., Jimenez, J.L., Canagaratna, M.R., Ulbrich, I.M., Ng, N.L., Worsnop, D.R. and Sun, Y. (2011). Understanding atmospheric organic aerosols via factor analysis of aerosol mass spectrometry: A review. *Anal. Bioanal. Chem.* 401: 3045–3067.
- Zhang, R., Khalizov, A., Wang, L., Hu, M. and Xu, W. (2012). Nucleation and growth of nanoparticles in the atmosphere. *Chem. Rev.* 112: 1957–2011.
- Zhang, R., Suh, I., Zhao, J., Zhang, D., Fortner, E.C., Tie, X., Molina, L.T. and Molina, M.J. (2004). Atmospheric new particle formation enhanced by organic acids. *Science* 304: 1487–1490.
- Zhang, R., Li, G., Fan, J., Wu, D.L. and Molina, M.J.

(2007). Intensification of Pacific storm track linked to Asian pollution. *Proc. Natl. Acad. Sci. U.S.A.* 104: 5295–5299.

Received for review, April 10, 2019

Revised, March 5, 2020

Accepted, March 6, 2020